

# Geophysical Research Letters

## RESEARCH LETTER

10.1029/2021GL093632

### Key Points:

- Coral bleaching exerts significant ecological and societal impacts in the western tropical Pacific Ocean
- Coral bleaching severity at Palau does not correspond simply to an El Niño-Southern Oscillation index, such as Niño-3.4
- Regional intrinsic ocean variability and pre-conditioning upper ocean thermal structures play critical roles

### Correspondence to:

B. Qiu,  
[bo@soest.hawaii.edu](mailto:bo@soest.hawaii.edu)

### Citation:

Qiu, B., Colin, P. L., & Chen, S. (2021). Time-varying upper ocean circulation and control of coral bleaching in the western tropical Pacific. *Geophysical Research Letters*, 48, e2021GL093632. <https://doi.org/10.1029/2021GL093632>

Received 30 MAR 2021  
Accepted 3 JUL 2021

## Time-Varying Upper Ocean Circulation and Control of Coral Bleaching in the Western Tropical Pacific

Bo Qiu<sup>1</sup> , Patrick L. Colin<sup>2</sup> , and Shuiming Chen<sup>1</sup> 

<sup>1</sup>Department of Oceanography, University of Hawaii at Manoa, Honolulu, HI, USA, <sup>2</sup>Coral Reef Research Foundation, Koror, Palau

**Abstract** The western tropical Pacific Ocean (WTPO) features complicated ocean circulation systems and has the warmest world open-ocean waters. Small upper ocean temperature change there can exert significant impact on the regional coral reef ecosystems. In the past three decades, moderate to severe coral bleaching events have been observed in the WTPO surrounding Palau in 1998, 2010, 2016, 2017, and 2020. Reflecting the diversity of El Niño-Southern Oscillation (ENSO) variability, the observed coral bleaching severity does not correspond simply to the amplitude of an ENSO index, such as Niño-3.4. By conducting an upper ocean temperature budget, we found the time-varying upper ocean circulation advection acted to damp the anomalous surface heat flux forcing and played critical roles in controlling the surface ocean thermal conditions around Palau. This happened either directly via the advective temperature flux convergence, or indirectly through the pre-conditioning of upper ocean thermal structures.

**Plain Language Summary** This study investigated the role of upper ocean circulation variability in modulating the ambient environment of coral reef ecosystems in the Western Tropical Pacific Ocean (WTPO), in particular, those leading to warming events that exceed the temperature threshold for coral bleaching around the island of Palau. Reef ecosystems rely on a relationship between the coral polyps and symbiotic algae that lives within the coral. Bleaching occurs when increased temperatures or environmental cause the algae to be expelled and unless the stress is removed the coral will die within weeks. Around Palau, moderate to severe coral bleaching occurred in 1998, 2010, 2016, 2017, and 2020. Combining in-situ water temperature data with analysis of the output from a data-assimilated ocean state estimate, we present evidence/results that the coral bleaching severity in the WTPO does not depend simply on the intensities of the conventional tropical El-Niño and La Niña events. Regional intrinsic ocean variability and upper ocean thermal structures pre-conditioned by the interannually-varying WTPO circulation both played critical roles in controlling the observed thermal stress levels for coral reefs around Palau.

## 1. Introduction

The western tropical Pacific Ocean (WTPO) is where many major low-latitude oceanic currents originate, bifurcate, and interact. The North Equatorial Current (NEC) flows westward, carrying wind-driven convergent Sverdrup transport across the interior Pacific (Figure 1a). After encountering the Philippine coast, the NEC bifurcates into the northward-flowing Kuroshio and the southward-flowing Mindanao Current (MC; Nitani, 1972; Qiu & Lukas, 1996). Part of the MC intrudes into the Celebes Sea and feeds the Indonesian Throughflow (ITF), and the remaining part veers eastward to form a component of the North Equatorial Countercurrent (NECC; Gordon & Fine, 1996; Kashino et al., 2001; Lukas et al., 1991). A similar situation also exists in the tropical South Pacific where, upon reaching the Australian coast, the westward-flowing South Equatorial Current (SEC) splits into the northward-flowing North Queensland Current and the southward-flowing East Australian Current (Kessler & Gourdeau, 2007; Roemmich et al., 2005). After passing by the Solomon Sea, the NQC connects to the New Guinea Coastal Current/Undercurrent (NGCC/UC) system. A part of the NGCUC peels off in the Bismarck Sea to form the eastward-flowing Equatorial Undercurrent (EUC) and some of its water continues northwestward and crosses the equator to contribute to the formation of the NECC and ITF (Fukumori et al., 2004; Gouriou & Toole, 1993; Johnson et al., 2002).

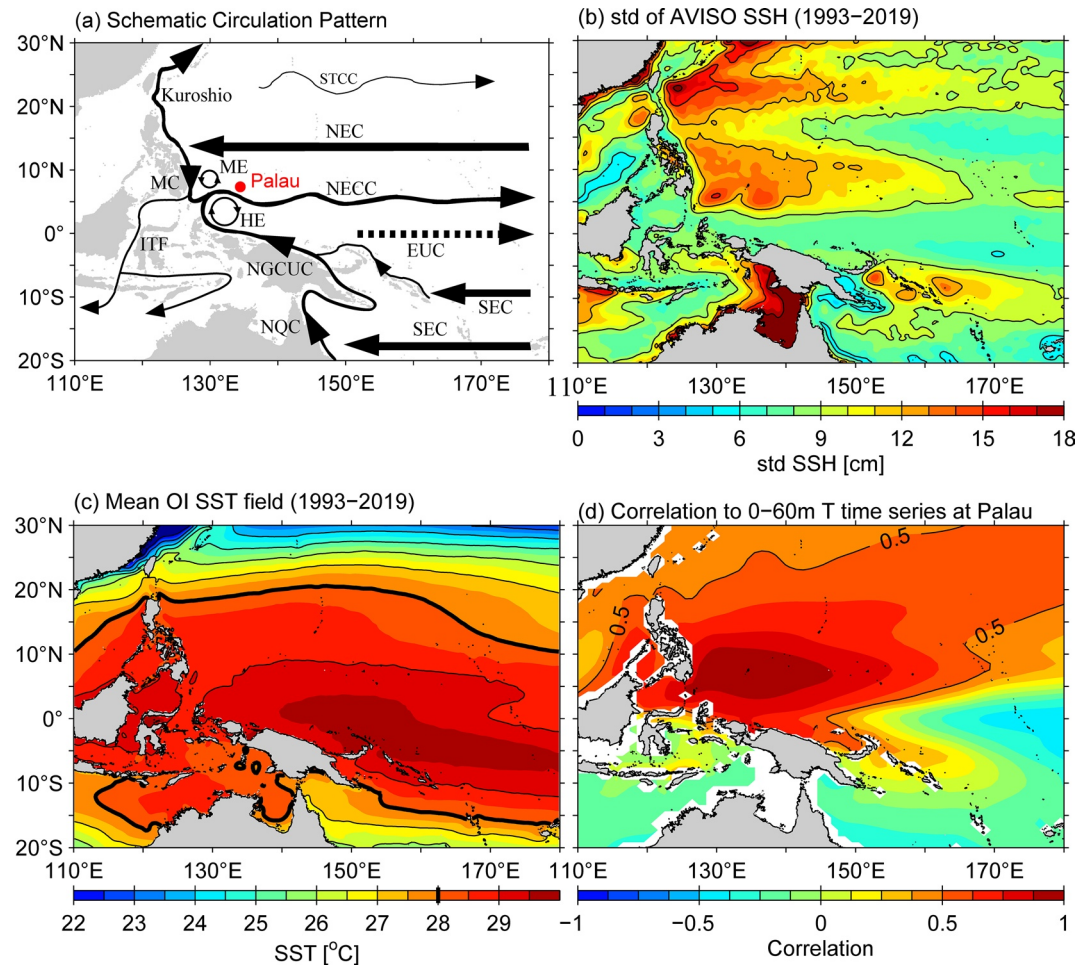


**Figure 1.** (a) Upper ocean circulation schematic in the western tropical Pacific Ocean. Currents shown are: Subtropical Countercurrent (STCC); North Equatorial Current (NEC); Mindanao Current (MC); Mindanao Eddy (ME); North Equatorial Countercurrent (NECC); Halmahera Eddy (HE); Indonesian Throughflow (ITF); Equatorial Undercurrent (EUC); New Guinea Coastal Undercurrent (NGCUC); South Equatorial Current (SEC); and North Queensland Current (NQC). (b) Sea surface height standard deviation map based on AVISO merged satellite altimeter data of 1993–2019. (c) Mean SST map of 1993–2019 based on OI-SST dataset of Reynolds et al. (2007). Solid thick contours denote the 28°C isotherms. (d) Correlation coefficient map of upper ocean (0–60 m) temperature variability relative to that at Palau based on ECCOv4r4 state estimate (i.e., gray line in Figure 2c).

The WTPO circulation described above is highly variable (Figure 1b) because not only is it influenced by the regional monsoonal wind forcing and intrinsic instabilities, but the oceanic circulation in the western basin is also subject to the perturbations originating in the eastern Pacific basin due to planetary Rossby wave propagation (Cabrera et al., 2015; Kessler & Cravatte, 2013; Qiu & Chen, 2012). Climatically, upper ocean circulation variations play important roles in mass and heat budget/balance in the WTPO and in regulating the warm pool evolution and the life cycle of ENSO (Borovikov et al., 2001; Vialard et al., 2001; Wang & McPhaden, 2001). For example, the time-varying NECC controls the convergent surface warm water from the warm pool to the east, and changes in the EUC transport can modulate the upper ocean stratification to which the eastern equatorial Pacific cold tongue sea surface temperature (SST) is sensitive. A comprehensive review on both regional and global climate by the WTPO variability can be found in Hu et al. (2015).

Defined commonly by the threshold water temperature  $>28^{\circ}\text{C}$ , the Pacific warm pool occupies a vast upper ocean region in the western Pacific from  $15^{\circ}\text{S}$  to  $18^{\circ}\text{N}$  (Figure 1c). As the warm pool migrates seasonally, its associated SST signals exhibit a well-defined annual cycle. At Palau ( $7.5^{\circ}\text{N}$ ,  $134.6^{\circ}\text{E}$ ) near the center of the warm pool, the seasonally-varying SST has a typical amplitude of  $2^{\circ}\text{C}$  (Figure 2a). Larger upper ocean temperature change, however, can occur in concert with the tropical ENSO variability. For example, the

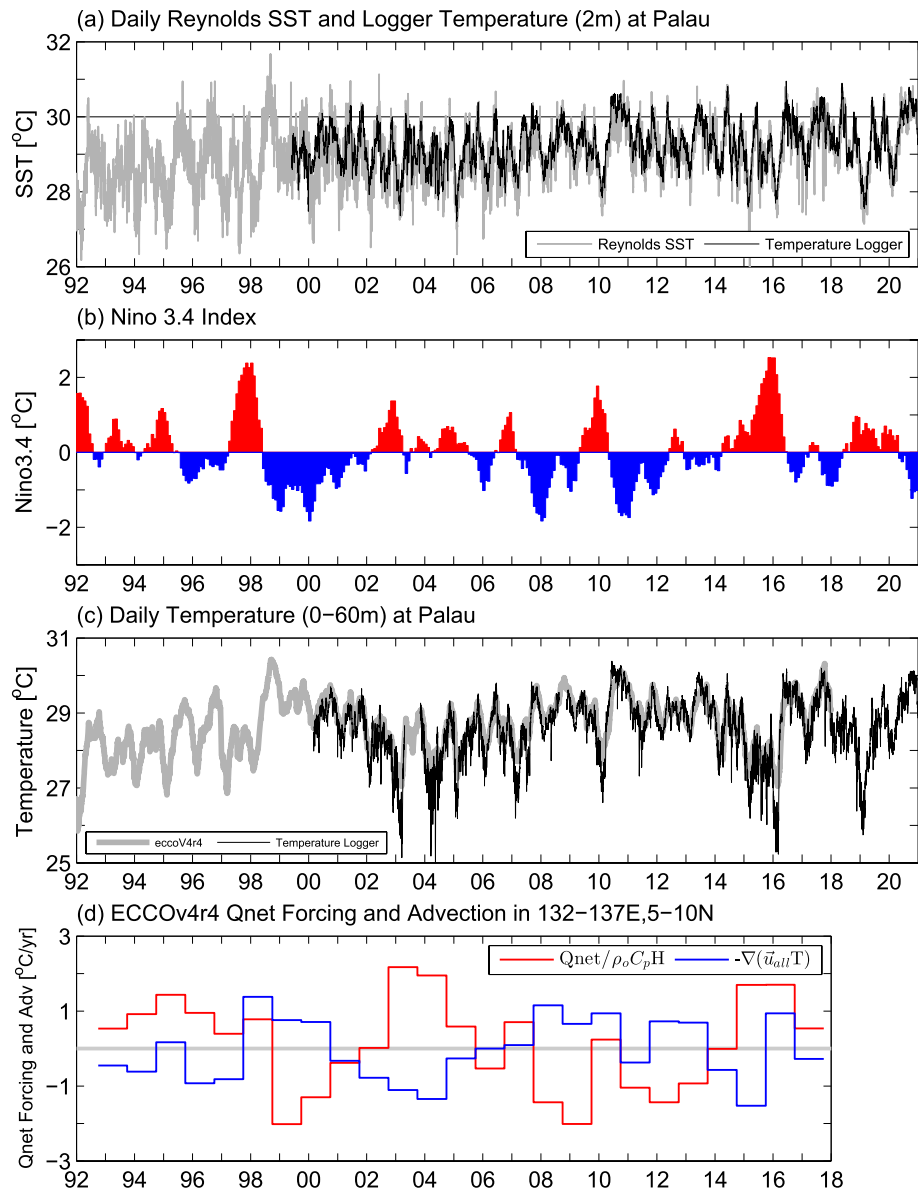


**Figure 2.** (a) Daily sea surface temperature (SST) time series at Palau (gray line) based on Reynolds et al. (2007) OI-SST dataset versus 2 m temperature logger time series (black line). Conditions above the 30°C threshold are considered conducive for coral bleaching. (b) Niño-3.4 index. (c) Daily upper ocean temperature in the 0–60 m layer around Palau from the temperature logger measurements (black line) and the ECCOV4r4 state estimate (gray line). (d) Yearly-mean surface net heat flux (red line) versus advective temperature flux convergence (blue line) anomaly time series in a  $5^{\circ} \times 5^{\circ}$  box surrounding Palau from ECCOV4r4. Here, yearly mean is taken from October of a previous year to September of the current year when seasonal upper ocean temperature values peak.

Palau SST in 1998 summer exceeded 31°C and was 5°C warmer than that in the preceding summer during the 1997 El Niño.

The SST variability in the WTPO exerts a profound impact on coral reefs and the ecosystems they support. Elevated upper ocean temperature imposes thermal stresses on corals and can lead to their bleaching, a condition where the symbiotic zooxanthellae algae found inside the cells of coral polyps are expelled, leaving the tissue largely colorless and the white coral skeleton visible (Colin, 2018; Hughes et al., 2018; Langlais et al., 2017). At Palau, corals were extensively bleached during summer 1998 with water temperatures >30°C from surface to 90 m depth and the mortality rate was estimated at 90% or more on the outer reef slopes (Figure 2a, Bruno et al., 2001; Colin, 2009). This bleaching episode followed the intense 1997 El

Niño event (Figure 2b). Coral bleaching at a reduced level compared to 1998 also occurred in 2010 at Palau (Schramek et al., 2018; van Woesik et al., 2012). Unlike 1998, however, this bleaching episode took place after the moderate El Niño of 2009. Following the super El Niño in 2015, severe coral bleaching was expected at Palau in 2016. After an initial moderate bleaching with the upper ocean hitting  $>30^{\circ}\text{C}$  in June, however, water temperatures dropped in summer 2016 associated with a westward propagating Rossby wave and no major bleaching was materialized (Colin, 2018; Qiu et al., 2019; Schönau et al., 2019). If we define the upper ocean thermal stress by integrating the observed 2 m temperature data (Figure 2a) exceeding  $30^{\circ}\text{C}$  over a calendar year, 1998 has a score of  $46.1^{\circ}\text{C}$  days, 2010 a score of  $52.9^{\circ}\text{C}$  days, and 2016 a score of  $16.6^{\circ}\text{C}$  days, respectively. During 1992–2020, two other years that have a score higher than 2016 are 2017 ( $21.6^{\circ}\text{C}$  days) and 2020 ( $50.0^{\circ}\text{C}$  days). Unlike in 1998, 2010, and 2016, neither 2017 nor 2020 was preceded by noticeable El Niño events (Figure 2c).

These above results suggest that the coral bleaching in the WTPO does not depend exclusively on the magnitude of the tropical ENSO variability and that other processes are likely at work and responsible for the evolution of the observed upper ocean thermal structures. This western tropical Pacific situation is in sharp contrast to the coral bleaching events in the central and eastern tropical Pacific where the bleaching severity is reported to be controlled predominantly by the strengths of El Niños (Barkley et al., 2018; Brainard et al., 2018). The objective of this study is to elucidate the physical processes responsible for the interannual upper ocean thermal structure variations that control the coral bleaching in the WTPO. Specifically, we will focus on diagnosis of upper ocean temperature budget and quantify the relative contributions from atmospheric forcing, advective oceanic forcing, and pre-existing oceanic circulation conditions leading to the observed high thermal stress events.

## 2. ECCO State Estimate

The Estimating the Circulation and Climate of the Ocean (ECCO) model uses the Massachusetts Institute of Technology general circulation model (MITgcm) that fits in a least squares sense to available satellite and in situ ocean observations after 1992 (Forget et al., 2015; Fukumori et al., 2021). The least squares fit is employed to adjust a number of model control parameters, including the surface forcing fields, initial conditions, and interior mixing coefficients. Using these adjusted control parameters, the model is run forward unconstrained as in other prognostic model simulations. Since no observational data are inserted in the forward integration, the ECCO state estimate is considered to be dynamically and kinematically consistent and well suited for exploring mechanisms of upper ocean temperature variability (Buckley et al., 2014; Wunsch & Heimbach, 2013). The ECCOv4r4 data set covers the period of 1992–2017 and has a horizontal resolution of  $\sim 0.8^{\circ}$  latitude  $\times$   $1^{\circ}$  longitude and a vertical resolution of 10 m in the upper WTPO of our interest. It is worth emphasizing that the upper ocean temperature variability from ECCOv4r4 agrees favorably with the observed upper ocean variability. As shown in Figure 2c, the observed versus simulated daily temperature time series in the 0–60 m upper ocean at Palau has a linear correlation coefficient  $R = 0.92$ .

## 3. Upper Ocean Temperature Budget Analysis

The governing equation for the upper-ocean temperature change can be written as follows:

$$\frac{\partial T}{\partial t} = -u \cdot \nabla T + \frac{1}{\rho C_p} \frac{\partial q}{\partial z} + K_h \nabla_h^2 T + \frac{\partial}{\partial z} \left( K_z \frac{\partial T}{\partial z} \right), \quad (1)$$

where  $u(u, v, w)$  is the three-dimensional velocity vector,  $q$  is surface heat flux,  $\rho$  is reference seawater density,  $C_p$  is specific heat of seawater,  $\nabla_h^2$  is the horizontal Laplacian operator, and  $K_h$  and  $K_z$  are the horizontal and vertical eddy diffusivity, respectively. Dynamically, the last two terms represent parameterized temperature diffusion due to unresolved horizontal/vertical turbulent processes in the ECCO state estimate.

To quantify the relative importance of various processes contributing to the SST changes, it is useful to integrate Equation 1 from sea surface down to a depth  $H$  that is, deeper than the local maximum mixed layer and then divide it by  $H$  (Qiu et al., 2017):

$$\frac{\partial}{\partial t} \left( \frac{1}{H} \int_{-H}^0 T dz \right) = -\frac{1}{H} \int_{-H}^0 \mathbf{u} \cdot \nabla T dz + \frac{Q_{\text{net}}}{\rho C_p H} + \left( \frac{K_h}{H} \int_{-H}^0 \nabla_h^2 T dz - \frac{K_z}{H} \frac{\partial T}{\partial z} \Big|_{z=-H} \right), \quad (2)$$

where  $Q_{\text{net}}$  denotes the net surface heat flux. Physically, LHS of Equation 2 indicates the time rate of change in averaged temperature in the upper ocean, the first term on RHS is the advective temperature flux convergence through the upper-ocean water column, the second term on RHS is the net heat exchange through the air-sea interface, and the last term in parentheses represents the diffusive temperature flux convergence. In ECCOV4r4, the background eddy diffusivity values are  $K_h = 10^3 \text{ m}^2/\text{s}$  and  $K_z = 10^{-1} \text{ m}^2/\text{s}$ . In the following analysis, we set  $H = 60 \text{ m}$  because it is the deepest regional mixed layer depth and because the majority of coral reefs around Palau grow in this upper ocean layer (Colin & Lindfield, 2019; de Boyer Montégut et al., 2004). For brevity, we denote below the temperature averaged in 0–60 m as  $T_{60\text{m}}$ . To evaluate the relative contributions to the interannual  $T_{60\text{m}}$  variability from the three processes on the RHS of Equation 2, we removed the linear trend and seasonal cycle over 1992–2017 from the daily ECCOV4r4 output and integrated Equation 2 over the two-year period encompassing the high thermal stress years of 1998, 2010, 2016 and 2017, and their respective preceding years. Due to lack of ECCOV4r4 output, no budget analysis is conducted for the 2020 high thermal stress event.

#### 4. Results

Following the severe coral bleaching event in 1998, a comprehensive temperature monitoring program was started in Palau by vertical arrays of temperature loggers that collected data from 2 to 90 m depth (Colin, 2018; Colin & Johnston, 2020). Figures 3b–3e show the observed upper ocean temperature time series in 2009–2010, 2015–2016, 2016–2017, and 2019–2020. For completeness, we also plot in Figure 3a the corresponding multi-depth temperature time series in 1997–1998 based on the ECCOV4r4 state estimate. As shown in Figure 2c, the ECCOV4r4 state estimate captures favorably the observed upper ocean temperature variability at Palau. One common feature detected in 1998, 2010, and 2016 is that reflecting the occurrence of El Niño in the preceding year, these years all started with low upper ocean temperatures in the 57–90 m layer. During March–April, all these three years experienced sharp increase in upper ocean temperatures on monthly timescales. The 90 m temperature in 2016, for example, jumped from 15 to 28°C within a short period of less than two months. Despite this common feature in rapid subsurface temperature warming, the summer SSTs in 1998, 2010, and 2016 evolved diversely, leading to different thermal stress conditions. The upper ocean temperature signals in 2017, on the other hand, exhibited characteristics very different from the three above-mentioned high thermal stress years. Only weak temperature modulations were observed at the 57 and 90 m depths. Rather than warming as in other high thermal stress year springs, 57 and 90 m temperatures decreased instead in spring of 2017. Upper ocean thermal structures in 2019–2020 evolved somewhat similarly to those in 2016–2017; a moderate El Niño took place in late 2018 and early 2019. Instead of summer 2019, high thermal stresses were detected in summer of 2020 (Figure 2c).

In light of these diverse upper ocean thermal structure evolutions, we conducted an upper ocean temperature budget analysis to evaluate and contrast the processes responsible for the high thermal stress conditions in 1998, 2010, 2016, and 2017. To do so, we used the ECCOV4r4 output and diagnosed relative roles played by the surface atmospheric heat forcing, oceanic advective convergence, and eddy diffusive convergence that contributed to the  $T_{60\text{m}}$  changes (Equation 2). Figure 3 (right column) shows the time series of the time-integrated  $T_{60\text{m}}$  budget averaged in a  $5^\circ \times 5^\circ$  box surrounding Palau ( $5\text{--}10^\circ\text{N}$ ,  $132\text{--}137^\circ\text{E}$ ) in (f) 1997–1998, (g) 2009–2010, (h) 2015–2016, and (i) 2016–2017, respectively. Without loss of generality, all terms in Equation 2 are set to zero at the beginning of the two-year period and the climatological seasonal signals have been removed to highlight the interannual variability.

It is instructive to examine first the high thermal stress events in 1998 and 2016 that followed the two strongest El Niño events in the past century (L'Heureux et al., 2017). During 1997, 2015 when the El Niño was in growing and maturing phase, Figures 3f and 3h reveal that changes in  $T_{60\text{m}}$  around Palau were relatively small (blue lines) and the warming effect by nonseasonal surface heat flux forcing (red lines) was offset by the cooling effect by the nonseasonal advective + diffusive flux convergences (green and gray lines). These upper ocean balances were altered in the following 1998 and 2016 La Niña years. In 1998, the nonseasonal

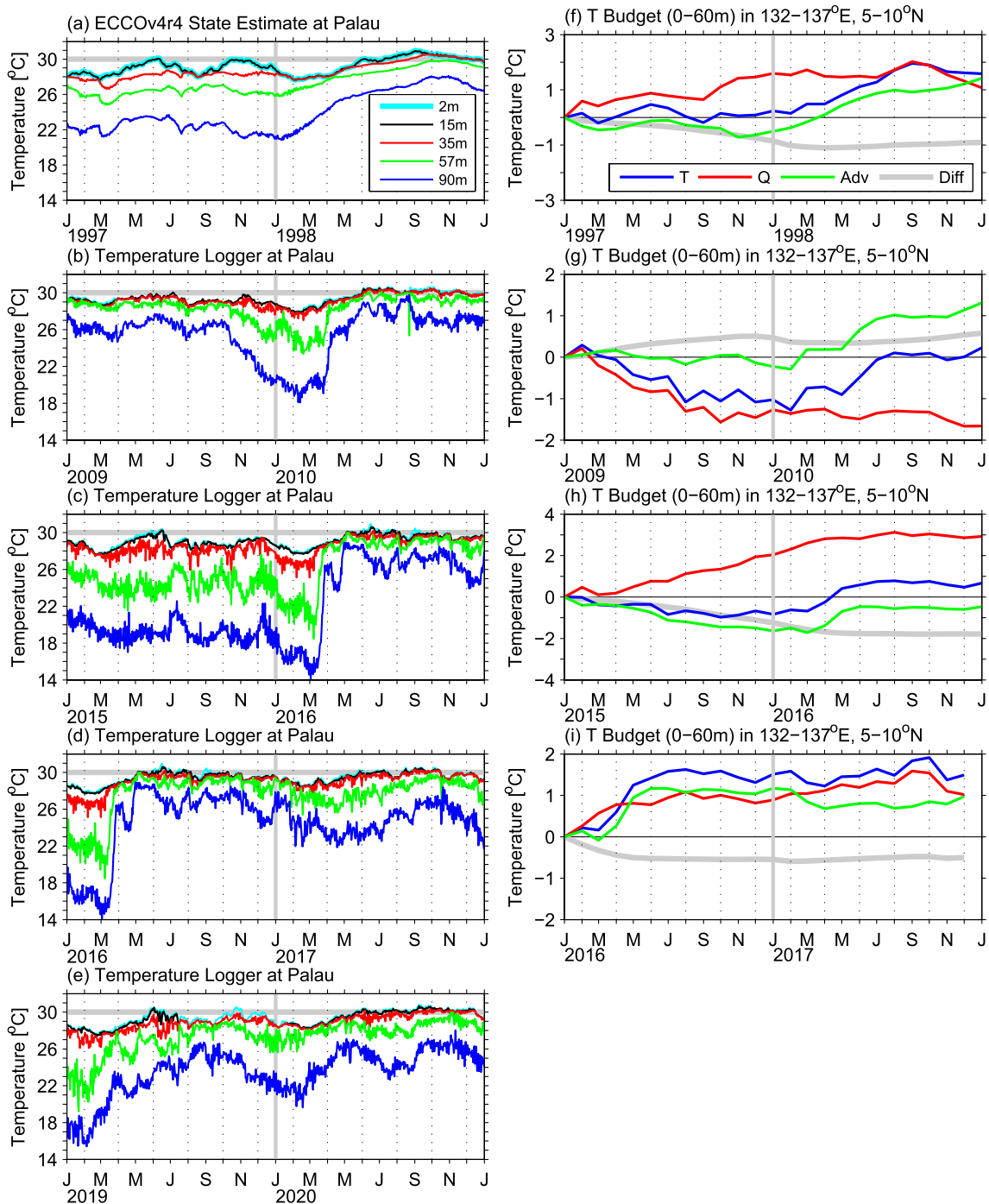


**Figure 3.** Left column: Daily upper ocean temperature time series off Palau from (a) ECCOv4r4 for 1997–1998, and (b–e) temperature logger measurements for 2009–2010, 2015–2016, 2016–2017, and 2019–2020, respectively. Right column: Time-integrated upper-ocean temperature budget over the period of (f) 1997–1998, (g) 2009–2010, (h) 2015–2016, and (i) 2016–2017 in the 132–137°E, 5–10°N region surrounding Palau. Blue lines denote the upper ocean temperature anomalies, red lines time-integrated surface heat flux forcing, green lines time-integrated advective flux convergence, and gray lines time-integrated diffusive flux convergence. Notice that the y-axis scales are different for the right-column four panels.

advective flux convergence worked to warm  $T_{60m}$  by as much as 2°C cumulatively and it explains much of the net 1.9°C warming in  $T_{60m}$ . Although smaller in amplitude, much of the 1.5°C warming in  $T_{60m}$  in 2016 was similarly due to the nonseasonal advective flux convergence forcing. In both 1998 and 2016, the weak warming effect by the nonseasonal surface heat input was counter-balanced by the cooling effect of the nonseasonal diffusive flux convergence.

In contrast to the eastern-Pacific (EP) El Niño in 1997, the El Niño event in 2009 is known as a central-Pacific (CP) type in which large-amplitude warm SST anomalies appeared near the dateline of the equatorial Pacific Ocean (Capotondi et al., 2015, 2020; Kao & Yu, 2009; Kug et al., 2009). The 2015 El Niño, on the other hand, has been categorized as a mixture of EP/CP types (Paek et al., 2017). Past studies have shown that the ocean circulation variability in the WTPO responds differently to the EP versus CP El Niños (Hsin & Qiu, 2012; Wang & Wu, 2013). This is indeed also the case for the upper ocean temperature budget surrounding Palau. As shown in Figure 3g, the 1°C decrease in  $T_{60m}$  in 2009 was mostly caused by the nonseasonal surface heat flux forcing and the advective/diffusive flux forcings played minor roles. These balances during the 2009 CP El Niño are very different from those diagnosed for 1997 and 2015. In the subsequent year 2010, the surface heat flux forcing is found to exert little effect and the 1.2°C warming in  $T_{60m}$  around Palau is by and large caused by the nonseasonal advective flux convergence forcing. This dominance of advection in controlling the  $T_{60m}$  variability is similar to the situation in 1998 and 2016 when the upper ocean temperature warming was similarly dictated by the advective flux convergence.

Unlike the above three high thermal stress years, 2017 was an ENSO neutral year. As indicated in Figure 3i, the nonseasonal advective heat flux convergence played a minor role in this year in modifying  $T_{60m}$  around Palau. With the benefit of starting from a warm upper ocean pre-conditioned by the 2016 warming,  $T_{60m}$  in 2017 increased progressively due to the anomalous heat input through the air-sea interface. Compared to 16.6°C days in 2016, the thermal stress at Palau reached a higher score of 21.6°C days in 2017. Dynamically, the 2017 event likely resulted from the weak 2016 La Niña condition that followed the 2015 El Niño, where a proper equatorial discharge was never accomplished.

## 5. Discussion

In conducting the upper ocean temperature budget analysis above, we have focused on  $T_{60m}$  at Palau whose interannual variations corresponded well to the regional thermal stress changes. It is worth emphasizing that the  $T_{60m}$  variability at Palau is representative of the thermal stress conditions for coral reefs across the broader WTPO. Figure 1d shows the spatial map of linear correlation coefficient ( $R$ ) between the  $T_{60m}$  variations at Palau (i.e., Figure 2c) and the neighboring WTPO. High correlation regions with  $R \geq 0.5$  are seen in the southern Philippine Sea (0–20°N and 120–170°E), the Celebes Sea, the Sulu Sea, and the region surrounding the Philippines. As such, understanding gained for the  $T_{60m}$  variations at Palau can be beneficial to the other parts of the WTPO. The fact that the high correlation values extend into the Celebes Sea, the Sulu Sea and the region surrounding the Philippines likely reflects the advective effects by the westward-branching MC and the poleward-flowing Kuroshio (see Figure 1a) that carry the interior ocean thermal stress signals into the marginal seas.

Our upper ocean temperature budget analyses revealed that the advective flux convergence forcing played a critical role in many instances in determining the  $T_{60m}$  evolutions. To gain further insights into what controls the advective flux convergence forcing under the interannually varying conditions in the WTPO, we plot in Figures 4b–4h the yearly upper ocean anomalous circulation maps in 1997–1998, 2009–2010, and 2015–2017. For reference, the long-term mean circulation map from the ECCOV4r4 product is shown in Figure 4a. In the 1997 and 2015 El Niño years, Figures 4b and 4f show that both the NEC and NECC intensified and migrated poleward in accordance with previous observational studies (Johnson et al., 2002; Qiu & Chen, 2010; Zhao et al., 2013). For the region surrounding Palau, this caused cold temperature advection from the subtropics and, as revealed in Figures 3f and 3h, the more enhanced NEC/NECC in 2015 resulted in stronger, negative advective flux convergence in 2015 than in 1997. Although the anomalous circulation of the NEC and NECC appeared similarly in the 1998 and 2016 La Niña years, the NECC weakened further and had a less equatorward migration in 1998 than in 2016 (cf. Figures 4c and 4g). As a result, a more pronounced positive advective flux convergence occurred in the WTPO that resulted in a warmer  $T_{60m}$  and

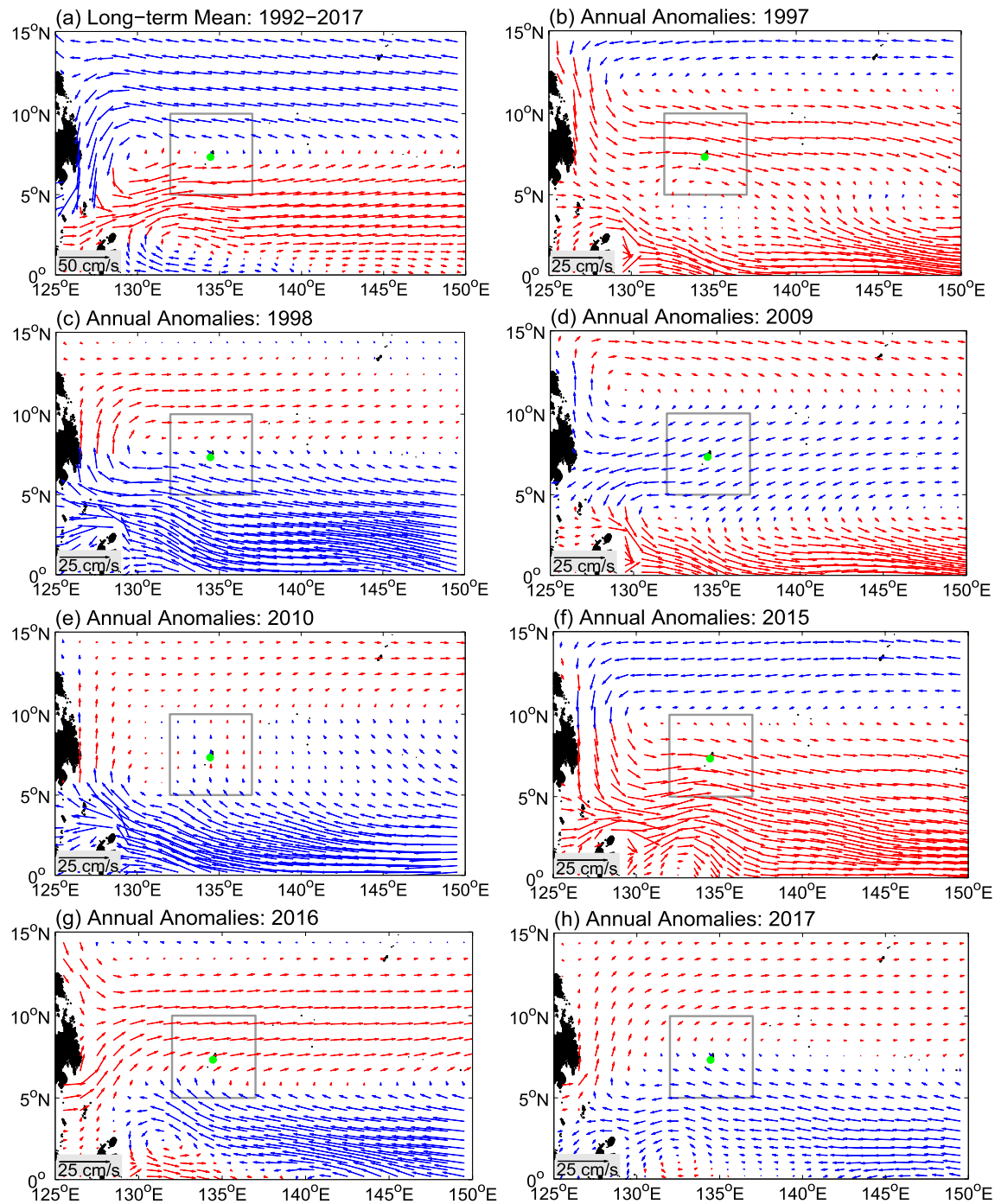


**Figure 4.** (a) Long-term mean field of 1992–2017. Annual mean anomaly fields in (b) 1997, (c) 1998, (d) 2009, (e) 2010, (f) 2015, (g) 2016, and (h) 2017. Velocity vectors with an eastward (westward) component are plotted in red (blue). The green dot denotes the location of Palau and gray box indicates the region wherein the upper ocean temperature budget is analyzed.

severe coral bleaching at Palau in 1998 than in 2016. Compared to 1997 and 2015, the NEC and NECC during the 2009 CP El Niño event exhibited very different anomalous features. As shown in Figure 4d, rather than strengthening, both the NEC and NECC weakened, resulting in weak advective flux convergence in 2009 as opposed to the large negative convergences detected in 1997 and 2015. In 2010, Figure 4e reveals that strong northwestward flows were generated along the equatorial band south of Palau. It is these anomalous

northwestward flows that brought warmer equatorial water northward, resulting in anomalously high  $T_{60m}$  and thermal stress values around Palau in 2010.

With 2017 being an ENSO neutral year, the upper ocean circulation anomalies were weak (Figure 4h), leading to an insignificant advective flux convergence forcing around Palau. The high upper ocean temperature value observed in September 2017, as we noted in the preceding section, was due to the warmer upper ocean state pre-conditioned in 2016. Since the warmer upper ocean states also occurred in the La Niña years of 1998 and 2010, a question arising naturally is why there were no pre-conditioned high thermal stress episodes in 1999 and 2011 similar to 2017. The answer to this question lies in the fact that the region around Palau in 1999 and 2011 were under anomalous surface cooling (see Figure 2d) that damped the warmer upper ocean conditions set up in the preceding years. Anomalous surface heating, on the other hand, prevailed around Palau in 2017 and this led to a higher thermal stress condition in its fall than in 2016 as diagnosed in Figure 3i.

A comparison between Figures 2b and 2d (red line) reveals that the surface heat flux forcing is highly correlated with the yearly-mean Niño-3.4 index at  $R = 0.77$ . However, as shown by the blue line in Figure 2d, the interannually-varying surface heat flux forcing is anti-correlated with the advective temperature flux convergence forcing at  $R = -0.54$ . Due to this anti-correlation, the  $\partial T_{60m}/\partial t$  term, which is controlled by the sum of these two forcings, shows a much lower correlation ( $R = 0.37$ ) with the Niño-3.4 index and is the reason why a simple ENSO index does not serve as a useful barometer for the upper ocean thermal stress conditions in the WTPO. In fact, each El Niño and La Niña event has been unique (Capotondi et al., 2015, 2020) and the different thermal stress conditions observed at Palau reflects the diversity of the ENSO phenomena existing in the tropical Pacific.

We have examined in this study the upper ocean temperature evolutions and budgets leading to the 1998, 2010, 2016, and 2017 high thermal stress events around Palau. A new such event took place in 2020 and it presented aspects of the upper ocean temperature evolutions reminiscent of the 2017 event based on currently available observations. It will be important for future studies to quantify if an upper ocean temperature budget similar to 2017 is at work and whether the on-going tropical Pacific warming alters the upper ocean temperature balances during the 2020 event.

## Data Availability Statement

The Palau Coral Reef Research Foundation (CRRF) maintains a public website <https://wtc.coralreefpalau.org/> that contains the in-situ temperature logger data used in this study. The daily ECCOV4r4 data is available at <https://ecco-group.org/products-ECCO-V4r4.htm>.

## Acknowledgments

Water temperature monitoring was supported by the Coral Reef Research Foundation and the Office of Naval Research "Flow Encountering Abrupt Topography" directive. The staff of CRRF is thanked for supporting field activities since 1999. B.Qiu and S.Chen acknowledge support from NASA's Physical Oceanography Program (80NSSC21K0552).

## References

- Barkley, H. C., Cohen, A. L., Mollica, N. R., Brainard, R. E., Rivera, H. E., De Carlo, T. M., et al. (2018). Repeat bleaching of a central Pacific coral reef over the past six decades (1960-2016). *Communications Biology*, 1, 177. <https://doi.org/10.1038/s42003-018-0183-7>
- Borovikov, A., Rienecker, M. M., & Schopf, P. S. (2001). Surface heat balance in the equatorial Pacific Ocean: Climatology and the warming event of 1994-95. *Journal of Climate*, 14, 2624-2641. [https://doi.org/10.1175/1520-0442\(2001\)014<2624:SHBITE>2.0.CO;2](https://doi.org/10.1175/1520-0442(2001)014<2624:SHBITE>2.0.CO;2)
- Brainard, R. E., Oliver, T., McPhaden, M. J., Cohen, A., Venegas, R., Heenan, A., et al. (2018). Ecological impacts of the 2015/16 El Niño in the Central Equatorial Pacific. *Bulletin of the American Meteorological Society*, 99, S21-S26. <https://doi.org/10.1175/bams-d-17-0128.1>
- Bruno, J. F., Siddon, C. E., Whiman, J. D., Colin, P. L., & Toscano, M. A. (2001). El Niño related coral bleaching in Palau, western Caroline Islands. *Coral Reefs*, 20, 127-136. <https://doi.org/10.1007/s003380100151>
- Buckley, M. W., Ponte, R. M., Forget, G., & Heimbach, P. (2014). Low-frequency SST and upper-ocean heat content variability in the North Atlantic. *Journal of Climate*, 27, 4996-5018. <https://doi.org/10.1175/jcli-d-13-00316.1>
- Cabrera, O. C., Villanoy, C. L., Alabia, I. D., & Gordon, A. L. (2015). Shifts in chlorophyll  $\alpha$  associated with the North Equatorial Current bifurcation latitude off eastern Luzon. *Oceanography*, 28(4), 46-53. <https://doi.org/10.5670/oceanog.2015.80>
- Capotondi, A., Wittenberg, A. T., Kug, J.-S., Takahashi, K., & McPhaden, M. J. (2020). ENSO diversity. In M. J. McPhaden, A. Santoso and W. Cai (Eds.), *AGU monograph "El Niño southern oscillation in a changing climate"*. <https://doi.org/10.1002/9781119548164.ch4>
- Capotondi, A., Wittenberg, A. T., Newman, M., Di Lorenzo, E., Yu, J.-Y., Braconnot, P., et al. (2015). Understanding ENSO diversity. *Bulletin of the American Meteorological Society*, 96, 921-938. <https://doi.org/10.1175/bams-d-13-00117.1>
- Colin, P. L. (2009). *Marine environments of Palau* (p. 414). Indo-Pacific Press. Retrieved from <http://coralreefpalau.org/wp-content/uploads/2017/04/Colin-PL-2009-Marine-Environments-of-Palau.pdf>
- Colin, P. L. (2018). Ocean warming and the reefs of Palau. *Oceanography*, 31(2), 126-135. <https://doi.org/10.5670/oceanog.2018.214>
- Colin, P. L., & Johnston, T. M. S. (2020). Measuring temperature in coral environments: Experience, lessons, and results from Palau. *Journal of Marine Science and Engineering*, 8, 0680. <https://doi.org/10.3390/jmse8090680>

- Colin, P. L., & Lindfield, S. J. (2019). Palau. In Y. Loya, K. Puglise, & T. Bridge (Eds.), *Mesophotic coral ecosystems* (pp. 285–299). Springer. [https://doi.org/10.1007/978-3-319-92735-0\\_16](https://doi.org/10.1007/978-3-319-92735-0_16)
- de Boyer Montégut, C., Madec, G., Fischer, A. S., Lazar, A., & Iudicone, D. (2004). Mixed layer depth over the global ocean: An examination of profile data and a profile-based climatology. *Journal of Geophysical Research*, 109, C12003. <https://doi.org/10.1029/2004JC002378>
- Forget, G., Campin, J.-M., Heimbach, P., Hill, C. N., Ponte, R. M., & Wunsch, C. (2015). ECCO version 4: An integrated framework for non-linear inverse modeling and global ocean state estimation. *Geoscientific Model Development*, 8(10), 3071–3104. <https://doi.org/10.5194/gmd-8-3071-2015>
- Fukumori, I., Lee, T., Cheng, B., & Menemenlis, D. (2004). The origin, pathway, and destination of Niño-3 water estimated by a simulated passive tracer and its adjoint. *Journal of Physical Oceanography*, 34, 582–604. <https://doi.org/10.1175/2515.1>
- Fukumori, I., Wang, O., Fenty, I., Forget, G., Heimbach, P., & Ponte, R. M. (2021). *Synopsis of the ECCO central production global ocean and sea-ice state estimate (version 4 release 4)*. <https://doi.org/10.5281/zenodo.4533349>
- Gordon, A. L., & Fine, R. A. (1996). Pathways of water between the Pacific and Indian oceans in the Indonesian seas. *Nature*, 379(6561), 146–149. <https://doi.org/10.1038/379146a0>
- Gouriou, Y., & Toole, J. (1993). Mean circulation of the upper layers of the western Pacific Ocean. *Journal of Geophysical Research*, 98(22), 495–520. <https://doi.org/10.1029/93jc02513>
- Hsin, Y.-C., & Qiu, B. (2012). The impact of Eastern-Pacific versus Central-Pacific El Niños on the North Equatorial Countercurrent in the Pacific Ocean. *Journal of Geophysical Research*, 117, C11017. <https://doi.org/10.1029/2012JC008362>
- Hu, D., Wu, L., Cai, W., Gupta, A. S., Ganachaud, A., Qiu, B., et al. (2015). Pacific western boundary currents and their roles in climate. *Nature*, 522, 299–308.
- Hughes, T. P., Anderson, K. D., Connolly, S. R., Heron, S. F., Kerry, J. T., Lough, J. M., et al. (2018). Spatial and temporal patterns of mass bleaching of corals in the Anthropocene. *Science*, 359(6371), 80–83. <https://doi.org/10.1126/science.aan8048>
- Johnson, G. C., Sloyan, B. M., Kessler, W. S., & McTaggart, K. E. (2002). Direct measurements of upper ocean currents and water properties across the tropical Pacific during the 1990s. *Progress in Oceanography*, 52, 31–61. [https://doi.org/10.1016/s0079-6611\(02\)00021-6](https://doi.org/10.1016/s0079-6611(02)00021-6)
- Kao, H., & Yu, J. (2009). Contrasting eastern-pacific and central-pacific types of ENSO. *Journal of Climate*, 22, 615–632. <https://doi.org/10.1175/2008jcli2309.1>
- Kashino, Y., Firing, E., Hacker, P., Sulaiman, A., & Lukiyango. (2001). Currents in the Celebes and Maluku Seas. *Geophysical Research Letters*, 28, 1263–1266. <https://doi.org/10.1029/2000gl011630>
- Kessler, W. S., & Cravatte, S. (2013). ENSO and short-term variability of the South Equatorial Current entering the Coral Sea. *Journal of Physical Oceanography*, 43, 956–969. <https://doi.org/10.1175/jpo-d-12-0113.1>
- Kessler, W. S., & Gourdeau, L. (2007). The annual cycle of circulation of the southwest subtropical Pacific, analyzed in an ocean GCM. *Journal of Physical Oceanography*, 37, 1610–1627. <https://doi.org/10.1175/jpo3046.1>
- Kug, J.-S., Jin, F.-F., & An, S.-I. (2009). Two types of El Niño events: Cold tongue El Niño and warm pool El Niño. *Journal of Climate*, 22, 1499–1515. <https://doi.org/10.1175/2008jcli2624.1>
- Langlais, C. E., Lenton, A., Heron, S. F., Evenhuis, C., Sen Gupta, A., Brown, J. N., & Kuchinke, M. (2017). Coral bleaching pathways under the control of regional temperature variability. *Nature Climate Change*, 7(11), 839–844. <https://doi.org/10.1038/nclimate3399>
- L’Heureux, M. L., Takahashi, K., Watkins, A. B., Barnston, A. G., Becker, E. M., Liberto, T. E. D., et al. (2017). Observing and predicting the 2015/16 El Niño. *Bulletin of the American Meteorological Society*, 88, 1363–1382. <https://doi.org/10.1175/BAMS-D-16-0009.1>
- Lukas, R., Firing, E., Hacker, P., Richardson, P. L., Collins, C. A., Fine, R., & Gammon, R. (1991). Observations of the Mindanao current during the western equatorial Pacific Ocean circulation study. *Journal of Geophysical Research*, 96, 7089–7104. <https://doi.org/10.1029/91jc00062>
- Nitani, H. (1972). Beginning of the Kuroshio. In H. Stommel, & K. Yoshida (Eds.), *Kuroshio: Its physical Aspects of the Japan current* (pp. 129–163). University of Washington Press.
- Paek, H., Yu, J. Y., & Qian, C. (2017). Why were the 2015/2016 and 1997/1998 extreme El Niño different? *Geophysical Research Letters*, 44, 1848–1856. <https://doi.org/10.1002/2016GL071515>
- Qiu, B., & Chen, S. (2010). Interannual-to-decadal variability in the bifurcation of the North Equatorial Current off the Philippines. *Journal of Physical Oceanography*, 40, 2525–2538. <https://doi.org/10.1175/2010jpo4462.1>
- Qiu, B., & Chen, S. (2012). Multi-decadal sea level and gyre circulation variability in the northwestern tropical Pacific Ocean. *Journal of Physical Oceanography*, 42, 193–206. <https://doi.org/10.1175/jpo-d-11-061.1>
- Qiu, B., Chen, S., Powell, B., Colin, P. L., Rudnick, D. L., Schonau, M. C., & Schönau, M. (2019). Nonlinear short-term upper ocean circulation variability in the tropical western Pacific. *Oceanography*, 32(4), 22–31. <https://doi.org/10.5670/oceanog.2019.408>
- Qiu, B., Chen, S., & Schneider, N. (2017). Dynamical links between the decadal variability of the Oyashio and Kuroshio Extensions. *Journal of Climate*, 30, 9591–9605. <https://doi.org/10.1175/jcli-d-17-0397.1>
- Qiu, B., & Lukas, R. (1996). Seasonal and interannual variability of the North Equatorial Current, the Mindanao Current and the Kuroshio along the Pacific western boundary. *Journal of Geophysical Research*, 101(12), 315–330. <https://doi.org/10.1029/95jc03204>
- Reynolds, R. W., Smith, T. M., Liu, C., Chelton, D. B., Casey, K. C., & Schlax, M. G. (2007). Daily high-resolution-blended analyses for sea surface temperature. *Journal of Climate*, 20, 5473–5496. <https://doi.org/10.1175/2007jcli1824.1>
- Roemmich, D., Gilson, J., Willis, J., Sutton, P., & Ridgway, K. (2005). Closing the time-varying mass and heat budgets for large ocean areas: The Tasman box. *Journal of Climate*, 18, 2330–2343. <https://doi.org/10.1175/jcli3409.1>
- Schönau, M. C., Wijesekera, H., Teague, W., Colin, P., Gopalakrishnan, G., Rudnick, D., et al. (2019). The end of an El Niño: A view from Palau. *Oceanography*, 32(4), 32–45. <https://doi.org/10.5670/oceanog.2019.409>
- Schramek, T. A., Colin, P. L., Merrifield, M. A., & Terrill, E. J. (2018). Depth-dependent thermal stress around corals in the tropical Pacific Ocean. *Geophysical Research Letters*, 45, 9739–9747. <https://doi.org/10.1029/2018gl078782>
- van Woesik, R., Houk, P., Isechal, A. L., Idechong, J. W., Victor, S., & Golbuu, Y. (2012). Climate-change refugia in the sheltered bays of Palau: Analogs of future reefs. *Ecology and Evolution*, 2, 2474–2484. <https://doi.org/10.1002/ece3.363>
- Vialard, J., Menkes, C., Boulanger, J.-P., Delecluse, P., Guilyardi, E., McPhaden, M. J., & Madec, G. (2001). A model study of oceanic mechanisms affecting equatorial Pacific sea surface temperature during the 1997–98 El Niño. *Journal of Physical Oceanography*, 31, 1649–1675. [https://doi.org/10.1175/1520-0485\(2001\)031<1649:AMSOOM>2.0.CO;2](https://doi.org/10.1175/1520-0485(2001)031<1649:AMSOOM>2.0.CO;2)
- Wang, L.-C., & Wu, C.-R. (2013). Contrasting the flow patterns in the equatorial Pacific between two types of El Niño. *Atmosphere-Ocean*, 51, 60–74. <https://doi.org/10.1080/07055900.2012.744294>
- Wang, W., & McPhaden, M. J. (2001). Surface layer temperature balance in the Equatorial Pacific during 1997–98 El Niño and 1998–99 La Niña. *Journal of Climate*, 14, 3393–3407. [https://doi.org/10.1175/1520-0442\(2001\)014<3393:SLTBIT>2.0.CO;2](https://doi.org/10.1175/1520-0442(2001)014<3393:SLTBIT>2.0.CO;2)

- Wunsch, C., & Heimbach, P. (2013). Dynamically and kinematically consistent global ocean circulation and ice state estimates. In G. Sie-  
dler, S. M. Griffies, J. Gould, and J. A. Church (Eds.), *Ocean circulation and climate: A 21st century perspective* (pp. 553–579). Academic  
Press. <https://doi.org/10.1016/b978-0-12-391851-2.00021-0>
- Zhao, J., Li, Y., & Wang, F. (2013). Dynamical responses of the west Pacific North Equatorial Countercurrent (NECC) system to El Niño  
events. *Journal of Geophysical Research*, 118, 2828–2844. <https://doi.org/10.1002/jgrc.20196>